Sensors & Diagnostics

COMMUNICATION

View Article Online
View Journal | View Issue

Cite this: *Sens. Diagn.*, 2024, **3**, 1247

Received 7th June 2024,
Accepted 10th July 2024

DOI: 10.1039/d4sd00193a

rsc.li/sensors

A CRISPR-amplified label-free electrochemical aptasensor for the sensitive detection of HbA1c†

Jianfeng Ma, Youwei Zheng, Yaoyao Xie, Dan Zhu, Lianhui Wang * and Shao Su *

Glycated hemoglobin (HbA1c) is a pivotal biomarker for the monitoring and early diagnosis of diabetes. The CRISPR-Cas system has fascinating application prospects in the next generation of biosensors due to its high specificity, efficiency, flexibility, and customization. Herein, a label-free electrochemical aptasensor was designed for the detection of HbA1c by combining the specific recognition ability of aptamers with the signal amplification effect of the CRISPR-Cas12a system. In the presence of HbA1c, the *cis–trans* cleavage ability of Cas12a protein was activated, causing the pre-formed probe DNA to be heavily cleaved and the electrochemical signal to increase. With CRISPR-assisted signal amplification, the developed electrochemical aptasensor can detect as low as 0.84 ng mL^{-1} HbA1c. Moreover, this aptasensor can detect 10 ng mL^{-1} HbA1c in 50% human serum due to its high selectivity, reproducibility, and long-term stability, which is lower than its physiological level in human blood samples. All results proved that the proposed aptasensor has a promising application in the early diagnosis and long-term monitoring of diabetes.

Introduction

Diabetes mellitus has gradually become a threat to public health, which brings a heavy economic burden to society and families.[1–4] According to the Global Burden of Disease Study 2021, the number of diabetes patients is estimated to reach 1.31 billion worldwide by 2050.[5] It is well-known that careful blood glucose management plays a vital role in reducing long-term complications of diabetes.[6,7] Therefore, rapid and accurate early diagnosis of diabetes attracts more and more scientists' attention. Compared to classical blood glucose, glycated hemoglobin (HbA1c) has been recognized as a crucial biomarker for the diagnosis of diabetes because it reflects the average glucose level over a 2- to 3-month period.[8–10] Moreover, the HbA1c concentration is not affected by diets, insulin levels and emotions. In general, the HbA1c and the HbA1c level (HbA1c%) in normal individuals are approximately 3–13 mg mL^{-1} and 4–6%, respectively.[11,12] Importantly, the American Diabetes Association (ADA) and the World Health Organization (WHO) have set a diagnostic threshold of HbA1c% ≥ 6.5% for the diagnosis of diabetes since 2009. Due to the rapid increase of diabetes, it is urgent to develop high-performance methods for HbA1c detection.

Compared with antibodies, aptamers are considered as ideal recognized units for the capture and detection of HbA1c due to their high chemical stability, ease of large-scale synthesis, and high binding affinity.[13] Among all methods for HbA1c detection, the use of electrochemical aptasensors has been proved as an efficient method due to their easy preparation, high selectivity and fast detection process.[14–16] To further improve the performance of electrochemical aptasensors for HbA1c detection, different signal amplification strategies have been introduced into the construction of electrochemical aptasensors. For example, E. Omidinia *et al.* utilized hierarchical gold architecture structure-decorated reduced graphene oxide (rGO) as an electrode modifier to amplify the electrochemical signal. The large surface area and high conductivity of these nanocomposites led to a low detection limit (1 nM) for HbA1c detection.[17] Similarly, Yang *et al.* used silver-doped hollow carbon spheres (Ag@HCS) as signal amplification probes to construct an electrochemical aptasensor for HbA1c detection. Due to the large specific surface area and superior electrical conductivity of Ag@HCS, the designed aptasensor can detect as low as 0.35 μg mL^{-1} HbA1c.[18]

Recently, clustered regularly interspaced short palindromic repeat (CRISPR) technologies have been considered as powerful tools for developing next-generation biosensors for biological molecule detection due to their high

State Key Laboratory of Organic Electronics and Information Displays & Jiangsu Key Laboratory of Smart Biomaterials and Theranostic Technology, Institute of Advanced Materials (IAM), Nanjing University of Posts and Telecommunications, 9 Wenyuan Road, Nanjing 210023, China. E-mail: iamlhwang@njupt.edu.cn, iamssu@njupt.edu.cn

† Electronic supplementary information (ESI) available. See DOI: https://doi.org/10.1039/d4sd00193a

specificity, efficiency, flexibility, and customization.[19–24] Similar to duplex-specific nuclease (DSN) and DNAzyme, the cleavage activity of the CRISPR-Cas system can be easily regulated.[25,26] Moreover, the CRISPR-Cas system easily couples with aptamers to construct high-performance aptasensors.[27–29] Nowadays, CRISPR-based aptasensors are employed to analyze proteins,[27] small molecules,[28] and metal ions[29] with satisfactory results. For example, Wang *et al.* established a fluorescence biosensor based on rolling circle amplification (RCA) and the CRISPR-Cas12a system for HbA1c detection. With the assistance of RCA, the CRISPR-based biosensor can detect 0.129 pg mL^{-1} HbA1c with high selectivity and fast detection time.[30] Inspired by the above studies, a label-free electrochemical aptasensor was designed for the sensitive detection of HbA1c by coupling the specific recognition ability of aptamers and the signal amplification effect of the CRISPR-Cas12a system. It should be noted that the combination of the *cis*- and *trans*-cleavage of the CRISPR-Cas12a system could obviously improve the analytical performance of the designed electrochemical aptasensor. In the presence of HbA1c, the cleavage activity of the CRISPR-Cas12a system was activated, leading to an outstanding increase in the electrochemical signal. By monitoring the changes of the electrochemical signal, the designed aptasensor can qualitatively and quantitatively analyze both HbA1c and HbA1c%.

Materials and methods

Materials and reagents

All DNA oligomers were synthesized by Sangon Biotech Co., Ltd. (Shanghai, China), and are listed in Table S1.† All chemicals and reagents are also recorded in the ESI.†

Preparation of the recognition probe

A double-stranded DNA (dsDNA) structure composed of the aptamer and its complementary strand served as a recognition probe for recognizing HbA1c. At first, the aptamer and its complementary strand was incubated in phosphate buffer (PB) at 95 °C for 5 min. Then, the product was gradually cooled to room temperature at a rate of 2 °C min^{-1}. Finally, the designed probe was stored in a refrigerator for sensing application.

Fabrication of the electrochemical aptasensor

Firstly, the designed recognition probe was incubated with 10 mM tris(2-carboxyethyl)phosphine (TCEP) in the dark for 1 h to reduce the disulfide bonds. Subsequently, a gold electrode was pre-treated according to a classical cleaning procedure.[31] After drying, the probe was assembled on the cleaned gold electrode surface *via* gold–sulfur (Au–S) bonding followed by incubation for 16 h at room temperature, which was defined as probe/Au. After washing and drying, 10 mM MCH was used to block the nonspecific remaining sites of probe/Au for 1 h at room temperature. Then, 8 μL different concentrations of HbA1c were incubated onto the electrode surface for 1 h at 37 °C. For the CRISPR-based signal amplification, the Cas12a–crRNA complex was incubated onto the electrode surface for 20 min at 37 °C to cleave the assembled dsDNA and single-stranded DNA (ssDNA).

Electrochemical impedance spectroscopy (EIS) and square wave voltammetry (SWV) measurements were used to characterize the preparation process and the analytical performance of this aptasensor. In this work, $[Fe(CN)_6]^{3-/4-}$ was used as a redox probe to monitor the detection process. It should be noted that the difference in current signals ($\Delta I = I_{HbA1c} - I_{no\ HbA1c}$) was used to evaluate the effect of signal amplification and the analytical performance of the electrochemical aptasensor. All electrochemical measurements were repeated at least 3 times.

Results and discussion

Design principle of the electrochemical aptasensor

As illustrated in Scheme 1, a label-free electrochemical aptasensor was designed for highly sensitive detection of HbA1c. At first, the HbA1c aptamer (Apt) and the complementary strand (cDNA) were pre-assembled into a dsDNA, which was used as a recognition probe to recognize and capture HbA1c. Expectedly, a slight increase in the electrochemical signal was observed after the recognition of HbA1c. The added HbA1c preferentially bound with Apt and promoted the dissociation of the dsDNA structure. As a result, the product of Apt-HbA1c was released from the electrode surface, resulting in the dsDNA assembled on the electrode surface becoming ssDNA (only cDNA immobilized on the electrode surface). At this point, the electron transfer between the electrode surface and $[Fe(CN)_6]^{3-/4-}$ was facilitated, leading to an increase in the electrochemical signal. By further introducing the CRISPR-Cas12a system, an amplified electrochemical signal was obtained. In this work, the designed Cas12a–crRNA complex could specifically recognize the retained cDNA. Meanwhile, the *cis*- and

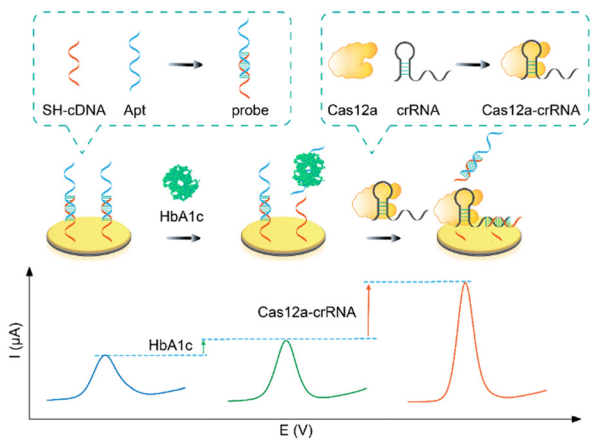

Scheme 1 Schematic illustration of a CRISPR-amplified electrochemical aptasensor for HbA1c detection.

trans-cleavage activity of Cas12a protein was activated. Therefore, both the assembled dsDNA and the retained ssDNA were cleaved, further facilitating the electron transfer between $[Fe(CN)_6]^{3-/4-}$ and the electrode surface to amplify the electrochemical signal.

Feasibility of the electrochemical aptasensor for HbA1c detection

The step-by-step assembly process of the electrochemical aptasensor is demonstrated in Fig. 1A. The construction process was characterized by electrochemical impedance spectroscopy (EIS) and square wave voltammetry (SWV). As displayed in Fig. 1B, the impedance value (R_{et}) of probe/Au (curve b, 1612 Ω) was larger than that of the bare gold electrode (curve a, 209 Ω), proving the successful immobilization of the probe on the electrode surface. As expected, the R_{et} of this electrochemical aptasensor significantly decreased with the addition of HbA1c (curve c, 1325 Ω). The reason was ascribed to the dissociation of dsDNA into ssDNA. When the CRISPR-Cas12a system was further introduced on the sensing surface, the R_{et} of the aptasensor further decreased (R_{et} = 848 Ω, curve *d*). The specific binding of cDNA and crRNA activated the *cis*- and *trans*-cleavage activity of Cas12a, leading to the cleavage of the assembled dsDNA and retained ssDNA. Therefore, the electron transfer between $[Fe(CN)_6]^{3-/4-}$ and the electrode surface became more convenient, resulting in a smaller impedance value. In addition, the feasibility of the electrochemical aptasensor for HbA1c detection was further validated by SWV. As shown in Fig. 1C, the bare Au electrode exhibits the highest oxidation peak current (26.03 μA, curve a). Obviously, the oxidation peak current of HbA1c/probe/Au (8.69 μA, curve c) is higher than that of probe/Au (6.31 μA, curve b). The reason is attributed to Apt in the probe which specifically recognizes HbA1c and disassociates from the electrode surface, facilitating electron transfer between the electrode and $[Fe(CN)_6]^{3-/4-}$. After introduction of the CRISPR-Cas12a system, the oxidation peak current of the Cas12a-crRNA/HbA1c/probe/Au further increased to 17.9 μA (curve d), which is attributed to the successful activation of the *cis*–*trans* cleavage activity of Cas12a. As a result, a large number of cDNAs and probes were cleaved. If the CRISPR-Cas12a system is introduced into probe/Au directly, the oxidation peak current shows almost no change (Fig. S1†), indicating that the CRISPR-based signal amplification is target-triggered. The above experimental results showed that the designed electrochemical aptasensor can effectively recognize and analyze HbA1c.

Evaluation of CRISPR-based signal amplification

As shown in Fig. 2, ΔI was used to evaluate the effect of the CRISPR-based signal amplification strategy. Obviously, the ΔI of the CRISPR-amplified aptasensor (Fig. 2B) is about 11.66 μA for 1 μg mL^{-1} HbA1c detection, which is about 4.4-fold that of no CRISPR-assisted aptasensor (CRISPR-free, Fig. 2A). The experimental results proved that CRISPR-based signal amplification can greatly enhance the analysis performance of the aptasensor.

The analytical performance of the electrochemical aptasensor

The critical experimental parameters of the electrochemical aptasensor were optimized to improve the analytical performance, and are recorded in Fig. S2.† Under the optimal conditions, the analytical performance of the CRISPR-free aptasensor and CRISPR-amplified aptasensor for HbA1c detection was tested, respectively. As shown in Fig. 3A and B, the currents of the CRISPR-free and CRISPR-amplified aptasensors increased with increasing concentrations of HbA1c, respectively. From the SWV curves of the CRISPR-free and CRISPR-amplified aptasensors, two linear relationships between the current change and the logarithm of HbA1c concentrations were obtained. The corresponding linear equations are $y = 2.663x + 2.776$ (R^2 = 0.988) and $y = 3.561x + 11.092$ (R^2 = 0.998), respectively (Fig. 3C). According to the equation, the detection limit of the CRISPR-amplified aptasensor was estimated to be 0.84 ng mL^{-1}, which is lower than some published works (Table S2†).[32–35] Compared with

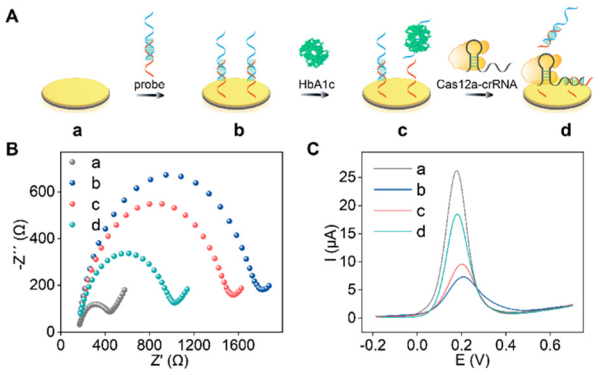

Fig. 1 (A) Schematics of the preparation process of the electrochemical aptasensor. (B) EIS and (C) SWV curves of (a) Au, (b) probe/Au, (c) HbA1c/probe/Au, and (d) Cas12a-crRNA/HbA1c/probe/Au in 0.5 mM $[Fe(CN)_6]^{3-/4-}$ solution containing 0.1 M KCl.

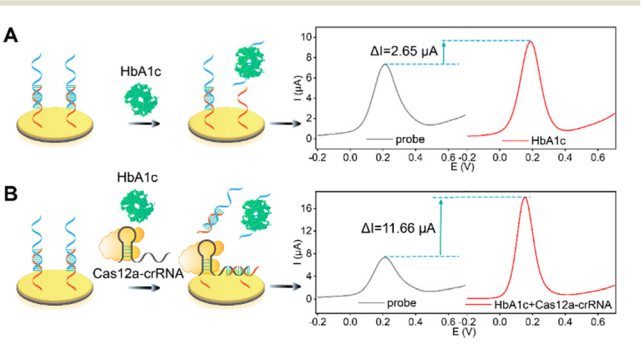

Fig. 2 Schematics and electrochemical signal change of the (A) CRISPR-free aptasensor and (B) CRISPR-amplified aptasensor for HbA1c detection in 0.5 mM $[Fe(CN)_6]^{3-/4-}$ solution containing 0.1 M KCl.

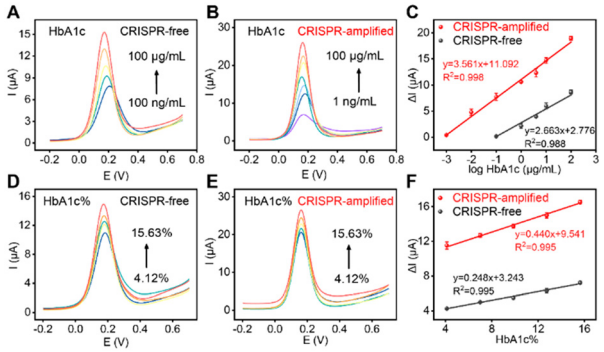

Fig. 3 (A) SWV curves of the CRISPR-free aptasensor for the detection of different concentrations of HbA1c. From bottom to top: 100 ng mL^{-1}, 1 μg mL^{-1}, 5 μg mL^{-1}, 10 μg mL^{-1} and 100 μg mL^{-1}. (B) SWV curves of the CRISPR-amplified aptasensor for the detection of different concentrations of HbA1c. From bottom to top: 1 ng mL^{-1}, 10 ng mL^{-1}, 100 ng mL^{-1}, 1 μg mL^{-1}, 5 μg mL^{-1}, 10 μg mL^{-1} and 100 μg mL^{-1}. (C) The linear relationships between the ΔI and the logarithm of HbA1c concentrations. (D) SWV curves of the CRISPR-free aptasensor for 4.12–15.63% HbA1c% detection. (E) SWV curves of the CRISPR-amplified aptasensor for 4.12–15.63% HbA1c% detection. (F) The linear relationships between the ΔI and the HbA1c%.

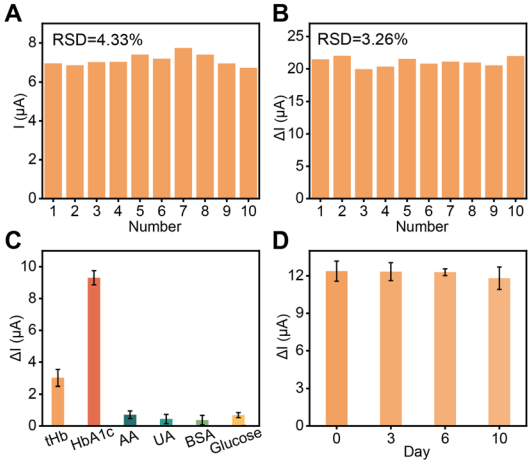

Fig. 4 (A) SWV responses of ten independent CRISPR-amplified aptasensors for HbA1c detection under the same conditions. (B) ΔI of ten independent CRISPR-amplified aptasensors for 100 μg mL^{-1} HbA1c detection. (C) ΔI of this aptasensor for the detection of tHb, HbA1c, AA, UA, BSA and glucose. (D) The storage stability of this aptasensor. The error bars represent the standard deviation of at least three independent measurements.

the CRISPR-free aptasensor, it can be seen that the CRISPR-amplified electrochemical aptasensor has a wider detection range (1 ng mL^{-1}–100 μg mL^{-1} *vs.* 100 ng mL^{-1}–100 μg mL^{-1}) and a lower limit of detection (0.84 ng mL^{-1} *vs.* 98 ng mL^{-1}) for HbA1c detection.

The designed aptasensor was also used to analyze HbA1c%. Fig. 3D and E show that the electrochemical signals of the CRISPR-free and CRISPR-amplified aptasensors increased with increasing HbA1c% in the range of 4.12–15.63%, respectively. Correspondingly, two linear relationships between the ΔI and HbA1c% were obtained for the CRISPR-free and CRISPR-amplified aptasensors with equations of $y = 0.248x + 3.243$ ($R^2 = 0.995$) and $y = 0.440x + 9.541$ ($R^2 = 0.995$), respectively (Fig. 3F). The detection limit of the CRISPR-amplified aptasensor for HbA1c% detection was estimated to be 0.01%, which is lower than that of the CRISPR-free aptasensor (0.98%). All experimental results suggested that our developed CRISPR-amplified label-free electrochemical aptasensor has a promising application in the early diagnosis of diabetes.

Reproducibility, selectivity and stability of the CRISPR-amplified aptasensor

The reproducibility was evaluated by using ten independent CRISPR-amplified aptasensors for 100 μg mL^{-1} HbA1c detection under the same conditions. The relative standard deviation (RSD) of the original current and ΔI was calculated to be 4.33% (Fig. 4A) and 3.26% (Fig. 4B), respectively, suggesting that this aptasensor has excellent reproducibility. Then, the selectivity of this electrochemical aptasensor was tested by selecting common biomolecules in the blood as interfering substances, including total hemoglobin (tHb), uric acid (UA), ascorbic acid (AA), bovine serum albumin (BSA), and glucose. As shown in Fig. 4C, no obvious electrochemical signal change of this CRISPR-amplified aptasensor was observed for UA, AA, BSA and glucose detection. Moreover, the ΔI of the CRISPR-amplified aptasensor for HbA1c detection was approximately 3 times higher than that for tHb, indicating that the aptasensor could effectively distinguish HbA1c and tHb. All results proved that the designed aptasensor can detect HbA1c with high selectivity. The long-term storage stability of this aptasensor was tested by placing the aptasensor in a refrigerator for different days. Fig. 4D shows no obvious decrease in ΔI after 10 days of storage, proving that this aptasensor has excellent storage stability.

Practical application of the CRISPR-amplified aptasensor

The practical application of this proposed aptasensor was evaluated by detecting various known concentrations of HbA1c (0.01, 0.1, 1 and 10 μg mL^{-1}) in 10%, 20% and 50% human serum. As shown in Fig. 5A–C, this aptasensor can accurately detect HbA1c in the complex samples with acceptable relative standard deviation (RSD, Tables S3–S5†). Although ΔI gradually decreased with the increase of human serum concentration, the proposed aptasensor could still detect 0.01 μg mL^{-1} HbA1c in 50% human serum (Fig. 5D and S3†), indicating that this aptasensor had a charming practical application in the early diagnosis and long-term monitoring of diabetes.

Conclusions

In this study, a CRISPR-amplified label-free electrochemical aptasensor was developed for the sensitive detection of HbA1c. Coupling the specific recognition ability of aptamers with the signal amplification effect of the CRISPR-Cas12a system, the designed electrochemical aptasensor exhibits

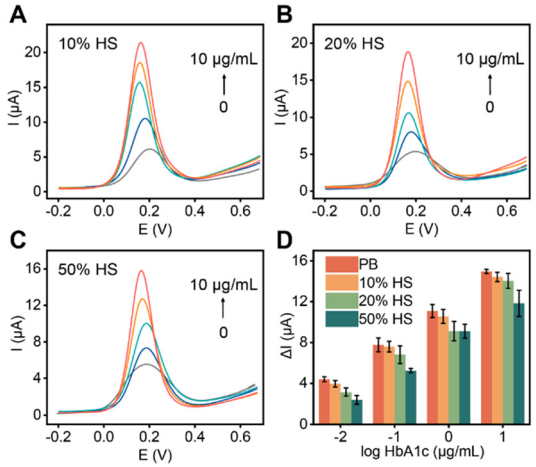

Fig. 5 SWV curves of this CRISPR-amplified aptasensor for the detection of different concentrations of HbA1c in (A) 10% human serum, (B) 20% human serum and (C) 50% human serum. (D) ΔI of the aptasensor was tested in PB, 10%, 20% and 50% human serum for the detection of 0.01, 0.1, 1 and 10 μg mL^{-1} HbA1c.

excellent sensitivity, reproducibility, selectivity, stability and anti-interference ability, which can be employed to analyze HbA1c in human serum samples. This electrochemical aptasensor is simple, sensitive, and low-cost, proving that it has good prospects in the early diagnosis and long-term monitoring of diabetes.

Author contributions

Jianfeng Ma: conceptualization, formal analysis, data curation, investigation, writing – original draft preparation. Youwei Zheng: methodology, validation, data curation, formal analysis. Yaoyao Xie: validation, data curation. Dan Zhu: methodology, formal analysis, visualization. Lianhui Wang: supervision, funding acquisition, project administration. Shao Su: writing – review and editing, supervision, funding acquisition, project administration.

Conflicts of interest

There are no conflicts to declare.

Acknowledgements

This work is supported by the Leading-edge Technology Program of Jiangsu Natural Science Foundation (BK20212012), the "Belt and Road" Innovation Cooperation Project of Jiangsu (BZ2022011), and the Natural Science Foundation of the Jiangsu Higher Education Institutions (22KJA150003).

Notes and references

1 L. Guariguata, D. R. Whiting, I. Hambleton, J. Beagley, U. Linnenkamp and J. E. Shaw, *Diabetes Res. Clin. Pract.*, 2014, **103**, 137–149.
2 A. J. M. Boulton, A. I. Vinik, J. C. Arezzo, V. Bril, E. L. Feldman, R. Freeman, R. A. Malik, R. E. Maser, J. M. Sosenko and D. Ziegler, *Diabetes Care*, 2005, **28**, 956–962.
3 J. M. Forbes and M. E. Cooper, *Physiol. Rev.*, 2013, **93**, 137–188.
4 A. Girach, D. Manner and M. Porta, *Int. J. Clin. Pract.*, 2006, **60**, 1471–1483.
5 K. L. Ong, *et. al.*, *Lancet*, 2023, **402**, 203–234.
6 N. A. ElSayed, G. Aleppo, V. R. Aroda, R. R. Bannuru, F. M. Brown, D. Bruemmer, B. S. Collins, J. L. Gaglia, M. E. Hilliard, D. Isaacs, E. L. Johnson, S. Kahan, K. Khunti, J. Leon, S. K. Lyons, M. L. Perry, P. Prahalad, R. E. Pratley, J. J. Seley, R. C. Stanton, R. A. Gabbay and A. American Diabetes, *Diabetes Care*, 2022, **46**, S19–S40.
7 A. American Diabetes, *Diabetes Care*, 2016, **40**, S11–S24.
8 S. Yazdanpanah, M. Rabiee, M. Tahriri, M. Abdolrahim, A. Rajab, H. E. Jazayeri and L. Tayebi, *Crit. Rev. Clin. Lab. Sci.*, 2017, **54**, 219–232.
9 I. M. Mostafa, H. Liu, S. Hanif, M. R. H. S. Gilani, Y. Guan and G. Xu, *Anal. Chem.*, 2022, **94**, 6853–6859.
10 Z. Zhan, Y. Li, Y. Zhao, H. Zhang, Z. Wang, B. Fu and W. J. Li, *Biosensors*, 2022, **12**, 221.
11 A. American Diabetes, *Diabetes Care*, 2007, **30**, S42–S47.
12 J. Yadav, A. Rani, V. Singh and B. M. Murari, *Biomedical Signal Processing and Control*, 2015, **18**, 214–227.
13 H.-M. Meng, H. Liu, H. Kuai, R. Peng, L. Mo and X.-B. Zhang, *Chem. Soc. Rev.*, 2016, **45**, 2583–2602.
14 S. H. Ang, M. Thevarajah, Y. Alias and S. M. Khor, *Clin. Chim. Acta*, 2015, **439**, 202–211.
15 C. Apiwat, P. Luksirikul, P. Kankla, P. Pongprayoon, K. Treerattrakoon, K. Paiboonsukwong, S. Fucharoen, T. Dharakul and D. Japrung, *Biosens. Bioelectron.*, 2016, **82**, 140–145.
16 L. Zhou, G. Figueroa-Miranda, S. Chen, M. Neis, Z. Hu, R. Zhu, Y. Li, M. Prömpers, A. Offenhäusser and D. Mayer, *Sens. Actuators, B*, 2023, **386**, 133730.
17 S. Y. Shajaripour Jaberi, A. Ghaffarinejad and E. Omidinia, *Anal. Chim. Acta*, 2019, **1078**, 42–52.
18 Y. Yang, H. Dong, H. Yin, J. Gu, Y. Zhang, M. Xu, X. Wang and Y. Zhou, *Bioelectrochemistry*, 2023, **152**, 108450.
19 M. M. Kaminski, O. O. Abudayyeh, J. S. Gootenberg, F. Zhang and J. J. Collins, *Nat. Biomed. Eng.*, 2021, **5**, 643–656.
20 Z. Weng, Z. You, J. Yang, N. Mohammad, M. Lin, Q. Wei, X. Gao and Y. Zhang, *Angew. Chem., Int. Ed.*, 2023, **62**, e202214987.
21 P. Fozouni, S. Son, M. Díaz de León Derby, G. J. Knott, C. N. Gray, M. V. D'Ambrosio, C. Zhao, N. A. Switz, G. R. Kumar, S. I. Stephens, D. Boehm, C.-L. Tsou, J. Shu, A. Bhuiya, M. Armstrong, A. R. Harris, P.-Y. Chen, J. M. Osterloh, A. Meyer-Franke, B. Joehnk, K. Walcott, A. Sil, C. Langelier, K. S. Pollard, E. D. Crawford, A. S. Puschnik, M. Phelps, A. Kistler, J. L. DeRisi, J. A. Doudna, D. A. Fletcher and M. Ott, *Cell*, 2021, **184**, 323–333.
22 M. Broto, M. M. Kaminski, C. Adrianus, N. Kim, R. Greensmith, S. Dissanayake-Perera, A. J. Schubert, X. Tan, H.

Kim, A. S. Dighe, J. J. Collins and M. M. Stevens, *Nat. Nanotechnol.*, 2022, **17**, 1120–1126.
23 J. S. Chen, E. Ma, L. B. Harrington, M. Da Costa, X. Tian, J. M. Palefsky and J. A. Doudna, *Science*, 2018, **360**, 436–439.
24 C. M. Ackerman, C. Myhrvold, S. G. Thakku, C. A. Freije, H. C. Metsky, D. K. Yang, S. H. Ye, C. K. Boehm, T.-S. F. Kosoko-Thoroddsen, J. Kehe, T. G. Nguyen, A. Carter, A. Kulesa, J. R. Barnes, V. G. Dugan, D. T. Hung, P. C. Blainey and P. C. Sabeti, *Nature*, 2020, **582**, 277–282.
25 H.-L. Shuai, K.-J. Huang, Y.-X. Chen, L.-X. Fang and M.-P. Jia, *Biosens. Bioelectron.*, 2017, **89**, 989–997.
26 J. Xu, Y. Liu, Y. Li, Y. Liu and K.-J. Huang, *Anal. Chem.*, 2023, **95**, 13305–13312.
27 Y. Dai, R. A. Somoza, L. Wang, J. F. Welter, Y. Li, A. I. Caplan and C. C. Liu, *Angew. Chem., Int. Ed.*, 2019, **58**, 17399–17405.
28 M. Liang, Z. Li, W. Wang, J. Liu, L. Liu, G. Zhu, L. Karthik, M. Wang, K.-F. Wang, Z. Wang, J. Yu, Y. Shuai, J. Yu, L. Zhang, Z. Yang, C. Li, Q. Zhang, T. Shi, L. Zhou, F. Xie, H. Dai, X. Liu, J. Zhang, G. Liu, Y. Zhuo, B. Zhang, C. Liu, S. Li, X. Xia, Y. Tong, Y. Liu, G. Alterovitz, G.-Y. Tan and L.-X. Zhang, *Nat. Commun.*, 2019, **10**, 3672.
29 Y. Xiong, J. Zhang, Z. Yang, Q. Mou, Y. Ma, Y. Xiong and Y. Lu, *J. Am. Chem. Soc.*, 2020, **142**, 207–213.
30 W. Wang, L. Geng, Y. Zhang, W. Shen, M. Bi, T. Gong, C. Liu, Z. Hu, C. Guo and T. Sun, *Microchem. J.*, 2024, **200**, 110370.
31 J. Zhang, S. Song, L. Wang, D. Pan and C. Fan, *Nat. Protoc.*, 2007, **2**, 2888–2895.
32 M. D. Mozammal Hossain, J.-M. Moon, N. G. Gurudatt, D.-S. Park, C. S. Choi and Y.-B. Shim, *Biosens. Bioelectron.*, 2019, **142**, 111515.
33 I. Pandey and J. D. Tiwari, *Sens. Actuators, B*, 2019, **285**, 470–478.
34 P. Zhang, Y. Zhang, X. Xiong, Y. Lu and N. Jia, *Sens. Actuators, B*, 2020, **321**, 128626.
35 A. Anand, C.-Y. Chen, T.-H. Chen, Y.-C. Liu, S.-Y. Sheu and Y.-T. Chen, *Nano Today*, 2021, **41**, 101294.